Investigation of diffusive grain interactions during equiaxed dendritic solidification

Abdelhalim Chirouf, Benoît Appolaire, Alphonse Finel, Yann Le Bouar, Miha Založnik

Investigation of diffusive grain interactions during equiaxed dendritic solidification

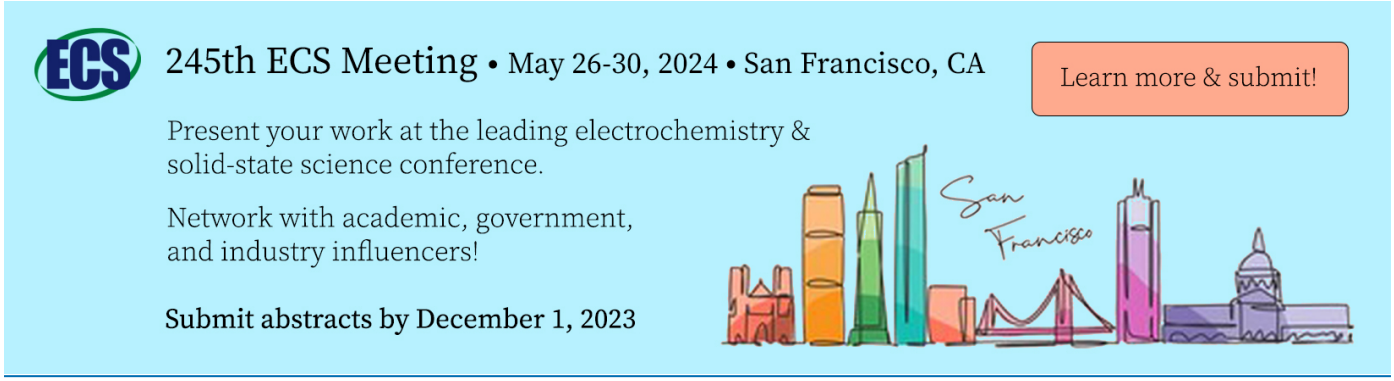

Investigation of diffusive grain interactions during equiaxed dendritic solidification

Abdelhalim Chirouf[1,2], Benoît Appolaire[1], Alphonse Finel[2], Yann Le Bouar[2], Miha Založnik[1]

[1] Université de Lorraine, CNRS, IJL, F-54000 Nancy, France
[2] Université Paris-Saclay, ONERA, CNRS, LEM, F-92322 Châtillon, France

E-mail: abdelhalim.chirouf@univ-lorraine.fr

Abstract. Grain growth during the solidification of an alloy is accompanied by the enrichment of the surrounding liquid phase in chemical species. The resulting diffusion fields induce interactions between the grains that are strongly dependent on their spatial arrangement. The influence of these diffusive interactions is not limited to the shapes and sizes of grains but also controls the overall kinetics of the transformation. In this study we investigate the role of the spatial arrangement of equiaxed grains in the average growth kinetics of an ensemble of grains. We perform full-field simulations of different grain ensembles using the mesoscopic grain envelope model (GEM). We show that the growth kinetics of randomly arranged ensembles is fundamentally different from that of periodic arrangements. We provide an explanation of this difference through analyses of the behaviour of individual grains in their local neighbourhood, defined by a Voronoi tessellation. Finally, we compare the full-field GEM simulations to state-of-the-art mean-field models and we point out the limitations of the latter in the prediction of dendritic growth.

1. Introduction

Modeling the solidification of metallic alloys can provide valuable insights into the microstructure of castings in various industrial processes, helping to optimize and improve these processes. One of the important phenomena to consider during solidification is the growth of equiaxed dendritic grains. During their growth, the liquid melt surrounding them is enriched in chemical species. Their growth is governed by the concentration field in their vicinity. When these grains are close to each other, their solute diffusion fields overlap, which leads to a modification of their growth kinetics [1, 2]. These interactions depend to a large extent on the spatial arrangement of the grains, in other words, they depend on how the grains are positioned relative to each other, especially in their close neighbourhood. Commonly used volume-averaged mean-field models for equiaxed solidification [3, 4] are based on overly simplistic assumptions on grain interactions. They describe them via ad hoc constitutive relations while ignoring the spatial arrangement aspect. Consequently, this limits their predictive capabilities.

In this paper, the aim is to highlight the influence of the spatial arrangement of equiaxed grains on their growth kinetics during solidification. Our approach consists in performing full-field numerical simulations of an ensemble of about 100 equiaxed grains using the grain envelope model (GEM) [5]. We compare simulation results for different grain arrangements, namely periodic and random arrangements and notice a major difference in terms of the overall growth

kinetics of an ensemble of grains. We then analyse individual grains in the ensemble and their interactions with their neighbourhood. Based on this analysis, we propose an explanation of the difference in behaviour between random and periodic arrangements. Furthermore, we highlight the shortcomings of state-of-the-art mean-field models in predicting growth, arising from the lack of consideration of grain arrangement.

2. Mesoscopic full-field simulations

2.1. Grain envelope model

The mesoscopic grain envelope model (GEM) [5, 6, 7] is a simulation tool for grain growth during solidification, developed with the aim to bridge the gap between microscopic and macroscopic solidification models. The description of dendrites by an envelope requires much coarser mesh in comparison to phase-field models since it does not describe the complexity of the solid-liquid interface. The envelope is a smooth hypothetical surface that connects the active dendrite branches, implying that there are both solid and liquid phases inside the envelope. The growth of the dendrites is determined by the movement of the envelope surface. The envelope velocity is given by a stagnant-film formulation of the Ivantsov solution for the dendrite tip velocity. This analytical solution relates the Péclet number of the tip to the local supersaturation in the liquid at a distance δ (the stagnant-film thickness) from the envelope. The supersaturation in the liquid outside the envelope (extragranular liquid) is obtained from the numerical solution of solute transport. The local supersaturation field in the vicinity of a grain is influenced by the solute enrichment caused by the growth of nearby grains. Therefore, the stagnant-film formulation accounts for the influence of solutal interactions between the grains on the envelope growth velocity. The liquid inside the envelope (intragranular liquid) is assumed to be at thermodynamic equilibrium and the fraction of the solid phase is calculated using a Scheil model.

2.2. Simulation parameters

We performed 3D numerical simulations of equiaxed grain growth during solidification of a binary alloy in isothermal conditions. The crystal structure has a cubic symmetry and dendrite branches growth along the $\langle 100 \rangle$ cubic directions. The physical parameters are the initial supersaturation, $\Omega_0 = \left(C_\mathrm{l}^* - C_0\right) / \left(C_\mathrm{l}^* - C_\mathrm{s}^*\right)$, and the grain density, N_V (i.e., the number of grains per unit volume). C_l^* and C_s^* are the liquid and solid equilibrium concentrations, respectively, and C_0 is the initial concentration of the liquid. Lengths are expressed in units of $L_\mathrm{diff} = D_\mathrm{l}/V_\mathrm{Iv}$, which is a characteristic diffusion length at the primary dendrite tip, where D_l is the diffusion coefficient in the liquid and V_Iv is the steady-state (Ivantsov) velocity of a primary dendrite tip growing into an infinite melt at a supersaturation Ω_0. The characteristic time is defined as $\tau = D_\mathrm{l}/V_\mathrm{Iv}^2$. The simulations were carried out for an initial supersaturation of $\Omega_0 = 0.05$ and for two grain densities, $N_V = 0.125 L_\mathrm{diff}^{-3}$ and $N_V = 0.35 L_\mathrm{diff}^{-3}$, called low and high density, respectively.

In order to highlight the influence of the spatial arrangement of the grains on the overall growth kinetics, we performed 4 simulations for each grain density: 3 with different periodic grain arrangements and one with a random grain arrangement. In the periodic cases, the grains were arranged in simple cubic (SC), body centred cubic (BCC) and face centred cubic (FCC) lattices with the $\langle 100 \rangle$ directions aligned with the cubic directions of the crystal lattice. The random cases had 125 grains, with both random positions and orientations. The grain arrangements are displayed in Fig. 1.

The stagnant-film thickness of the GEM is $\delta = 0.2 L_\mathrm{diff}$ and we used a regular discretisation grid with a mesh spacing $\Delta x = L_\mathrm{diff}/10$. All grains are initialised at $t = 0$ by spherical envelopes of radius $R_0 = 0.3 L_\mathrm{diff}$ and the simulation domain walls were considered to be symmetry planes.

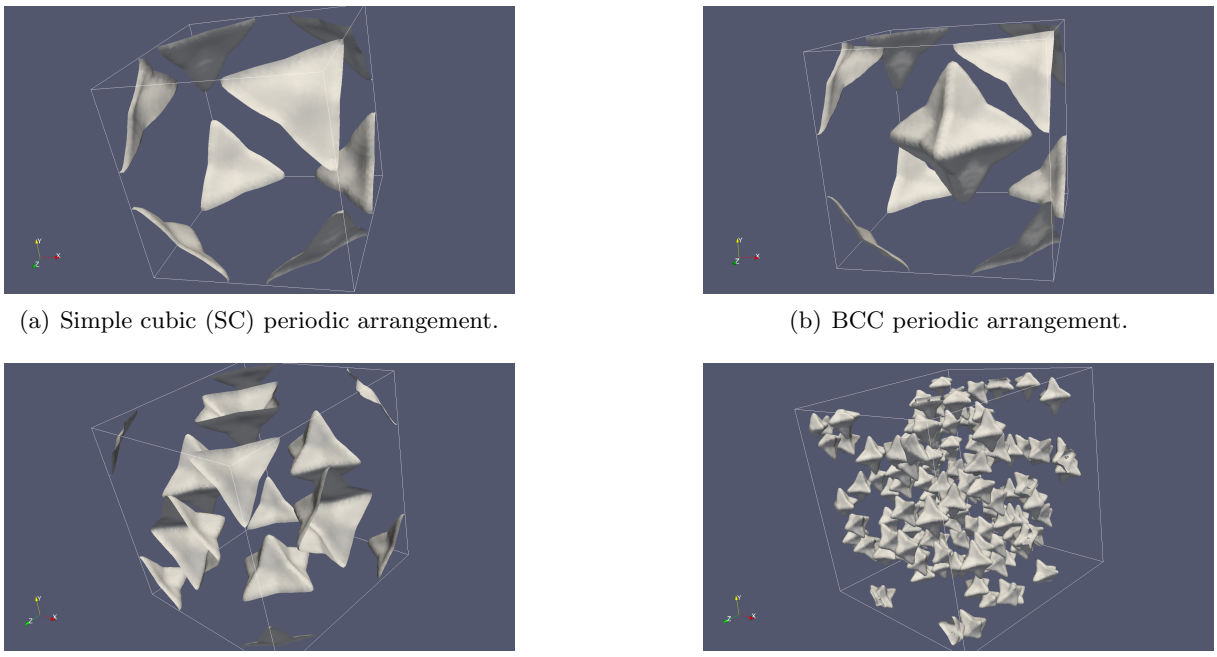

(a) Simple cubic (SC) periodic arrangement.

(b) BCC periodic arrangement.

(c) FCC periodic arrangement.

(d) Random arrangement.

Figure 1. Spatial arrangements of grains used in the simulations.

3. Simulation results

In this section we compare the evolution of average quantities of the ensembles for periodic and random arrangements. The link between the average quantities can be represented by the global solute mass balance, written in dimensionless form as:

$$g_e \frac{\partial \langle \Omega \rangle}{\partial t} = -\langle \Omega \rangle \frac{\partial g_e}{\partial t} + \frac{1}{V_0} j_S \tag{1}$$

where $\langle \Omega \rangle$ is the average supersaturation in the extragranular liquid, g_e is the extragranular liquid fraction and V_0 is the dimensionless volume of the system. The solute flux j_S diffusion from the grains to the extragranular liquid is given by:

$$j_S = -\int_{S_{\text{env}}} \vec{\nabla}\Omega \cdot d\vec{S} \tag{2}$$

where S_{env} is the surface of the envelopes in the system, and $d\vec{S}$ points outward from the envelopes.

In the GEM, the evolution of the envelope fraction is related to the tip velocity. Then, the evolution of the average supersaturation $\langle \Omega \rangle$ is given by the solute balance Eq. (1) and results from both the envelope growth and the solute flux diffusion from the grains to the extragranular liquid.

To compare the growth of crystalline grains with different initial grain arrangements, we will first examine the evolution of the average size of the grain envelopes. Next, we will investigate the average supersaturation in the extragranular liquid, as it plays a key role in determining the growth kinetics. Lastly, we will look at the average solute flux density across the grain envelopes to understand its impact on the evolution of the solute supersaturation in the extragranular liquid.

3.1. Average grain size

The average grain size is expressed as the radius of a sphere whose volume is equal to the envelope volume. The evolution of this quantity is shown in Fig. 2. For any given grain density, the increase of the equivalent radius is much slower for the random arrangement. When comparing two grain densities, we note faster growth for the lower density. As expected, the final equivalent radius is larger for the lower grain density.

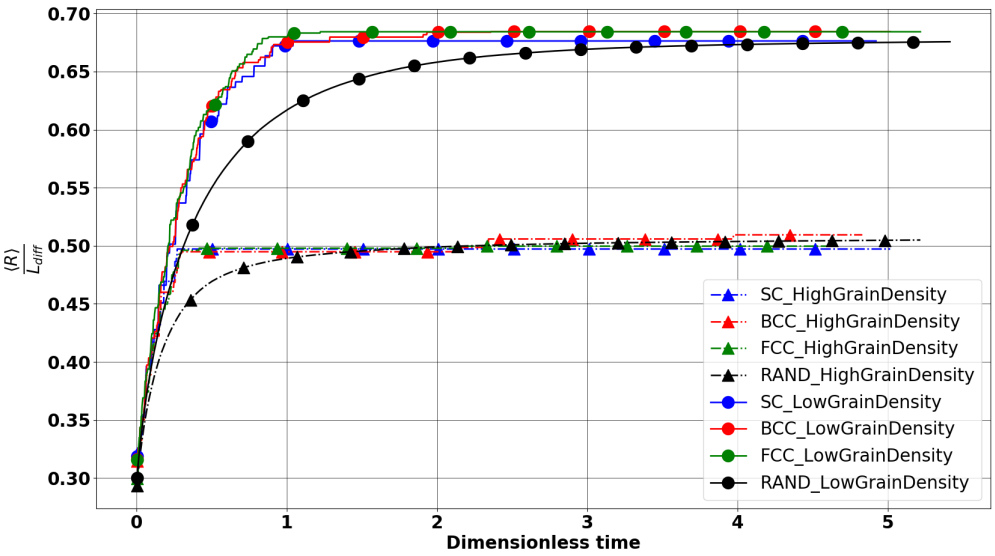

Figure 2. The evolution of the equivalent radius for different spatial arrangements of grains: SC (blue), BCC (red), FCC (green), and random (black). Low and high grain densities are indicated by circular and triangular symbols, respectively. The systems sizes in terms of edge length for the high density are: SC(1.41Ldiff), BCC(1.78Ldiff), FCC(2.23Ldiff), random(7.07Ldiff) for the low grain density the length of every edge is multiplied by $2^{1/2}$

3.2. Average supersaturation

The average supersaturation in the extragranular liquid evolves from the initial supersaturation $\Omega_0 = 0.05$ and decreases gradually to zero. The evolution is shown in Fig. 3. It appears that the lower the grain density the slower the decrease of the average supersaturation, regardless of the arrangement. In addition, for a given grain density, the decrease of the supersaturation is much slower in the random arrangement than in the periodic arrangements. The systems with BCC and FCC arrangements have almost identical evolutions. Only a slight difference is observed for the system with SC arrangement, for which the growth direction of the dendrites is towards the first neighbours of the grain arrangement. We also note that this difference is more pronounced for the low grain density.

3.3. Average solute flux density

We now compute the average solute flux density j_S/S_{env} diffused from the envelopes to the extragranular liquid using Eq. 2. The result is presented in Fig. 4. As expected, we observe a decrease of the flux density. The serrations, related to the discretization of the GEM model, do

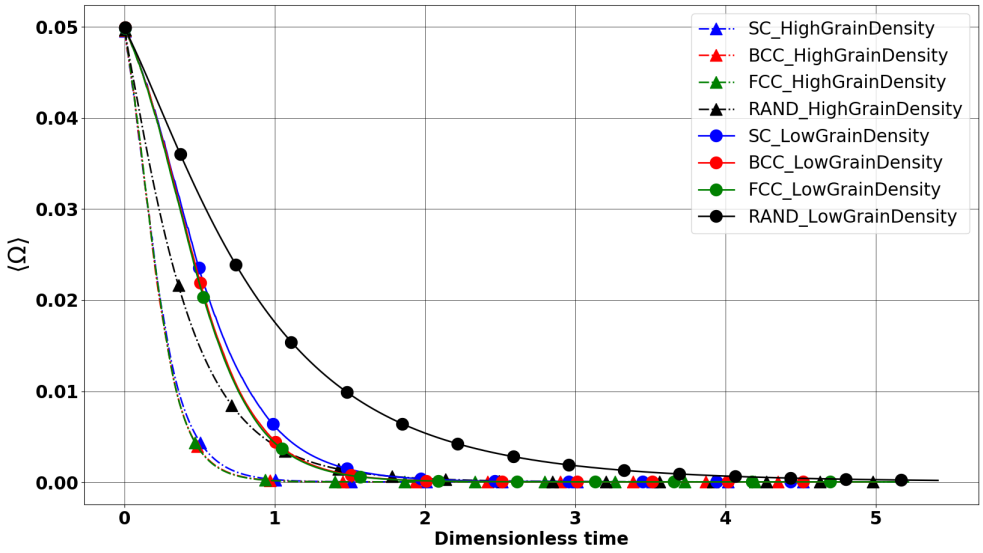

Figure 3. The evolution of the average supersaturation in the extragranular liquid for different spatial arrangements of grains: SC (blue), BCC (red), FCC (green), and random (black). Triangle mark for high grain density and circle for low grain density.

not hinder the comparison between the different cases under study and will not be discussed in this paper.

Comparing this flux density for different grain arrangements and a given grain density, we notice a slightly weaker flux density for the random arrangement. Subsequently this tendency is reversed and the flux density becomes higher for the random arrangement. Moreover, if we compare two grain densities for the same arrangement, we notice a stronger flux density for the lower grain density.

Overall, we notice that ensembles with a random arrangement of grains evolve differently from those with periodic arrangements. This disparity is due to the influence of grain arrangement on diffusive interactions between the grains. In the next section we present an analysis of individual grains in order to explain the origin of these differences.

4. Investigation of individual grains in a random arrangement

In a periodic grain arrangement all grains have exactly the same environment and their growth is therefore identical and equal to the global average. In a random arrangement, on the other hand, each grain has a different environment and grows differently in terms of size and shape. The results in the preceding section show that the overall (average) growth kinetics of the randomly arranged ensemble is not equivalent to that of a single grain with a size equal to the ensemble average. In this section we analyse the growth of individual grains in an attempt to gain understanding on how the contributions of individual grains result in the behaviour of the ensemble.

4.1. The range of interactions during growth

To analyse individual grains, we first need to define the environment that affects their growth. All grains interact via the diffusion field in the liquid, but we expect that the influence of

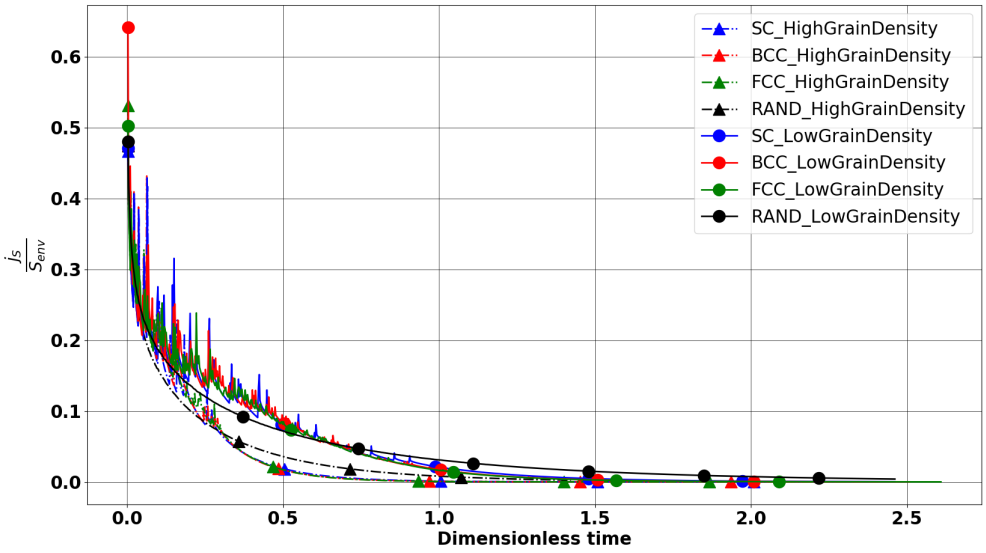

Figure 4. The evolution of the dimensionless global average solute flux density for different spatial arrangements of grains: SC (blue), BCC (red), FCC (green), and random (black). Low and high grain densities are indicated by circular and triangular symbols, respectively.

distant grains is screened off by closer grains. As a consequence, we expect that the strongest interactions are with the first nearest neighbour grains and we will focus on these interactions.

A convenient way to define the nearest neighbours is by a Voronoi tessellation constructed from the initial grain seeds. A Voronoi cell's nearest neighbors are those that share common cell faces. This space decomposition method is an effective way to define the local environment of grains, as the Voronoi cell of a grain represents the region of points that are closer to that grain than to any other grain. Furthermore, faces of a Voronoi cell are halfway between the neighboring grains and therefore the diffusion flux over the cell faces can be expected to be small. In order to test the validity of this assumption, we have calculated the solute flux densities across the Voronoi cell faces for each grain. Figure 5 shows the evolution of these flux densities for four different cells.

By comparing these solute flux densities to those from the grain envelopes to the extragranular liquid within the Voronoi cells, we can conclude that the solute exchange between Voronoi cells is insignificant. This can be attributed to the fact that the solute diffused by each pair of neighboring grains reaches the shared Voronoi cell face at approximately the same time. As the solute fluxes arriving at this face have similar magnitudes and are in opposite directions, they result in a negligible perpendicular component.

Because the solute flux across the Voronoi cell faces is negligible, we can consider each Voronoi cell to be independent from the rest of the system. Hence, We can consider that the interaction of a grain with the ensemble depends on its Voronoi cell volume. For instance, the larger the cell the weaker the interaction since the solute enrichment caused by the grain growth diffuses into a larger volume of liquid. Consequently, the solute concentration in the vicinity of the grain increases more slowly, resulting in a weaker impact on the concentration gradient at the envelope. This is corroborated by the observations we have made in the previous section on the influence of grain density on the evolution of the average supersaturation.

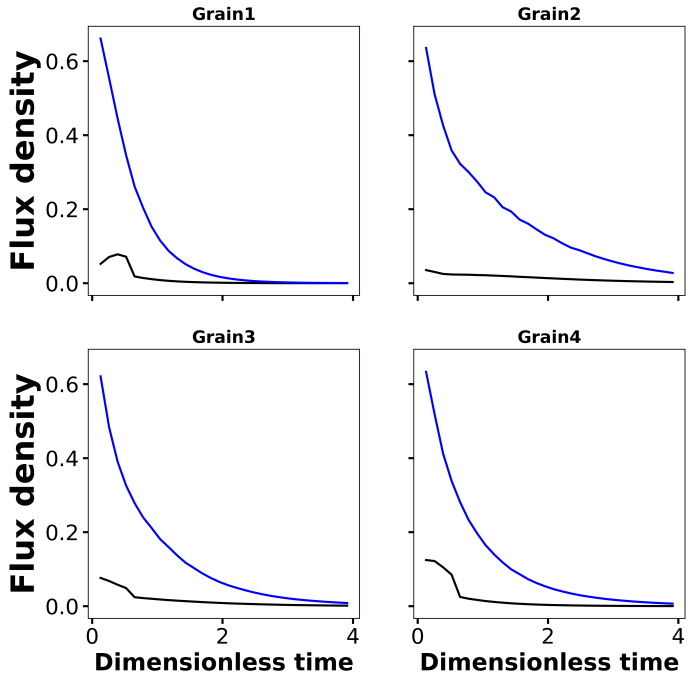

Figure 5. The evolution of the average solute flux density from the grain to the extragranular liquid inside the cell (blue) and of the average solute flux density across cell faces (black). These extractions were made on the low grain density simulation.

4.2. The evolution of individual grains

In order to highlight the disparity in behaviour among randomly dispersed grains, we have extracted the evolutions of the grain envelope size in terms of equivalent radius (Fig. 6) and of the average supersaturation in the extragranular liquid (Fig. 7), for the grains with the largest and the smallest Voronoi cells.

We observe a significant difference between grains within the largest and smallest cells. The grain in the largest cell exhibits faster growth and attains a larger final size. Conversely, the average supersaturation in the smallest cell drops rapidly, leading to an early attainment of equilibrium. Despite the stronger interactions with neighboring grains resulting in slower growth for the grain in the smallest cell, the liquid within the cell reaches equilibrium quickly, ultimately halting growth.

This is due to the fact that the time needed for the solute to diffuse within a cell of diameter L, scales as L^2. Therefore, as there is essentially no flux between the cells, the time needed for a cell of diameter L to reach equilibrium should approximately scale as L^2. This is in agreement with a simple analysis of Fig. 6 and Fig. 7. Indeed, if we note R_1 the final grain size in the smallest cell, we observe that the average final grain size is close to $2R_1$ and the final grain size in the largest cell is close to $3R_1$. These size relations that reflect the size relations between the corresponding cells, should lead to equilibrium times for the average and largest cells which are, respectively, approximately 4 times and 9 times larger than the the one observed for the smallest cell. This is indeed what we observe in Fig. 7.

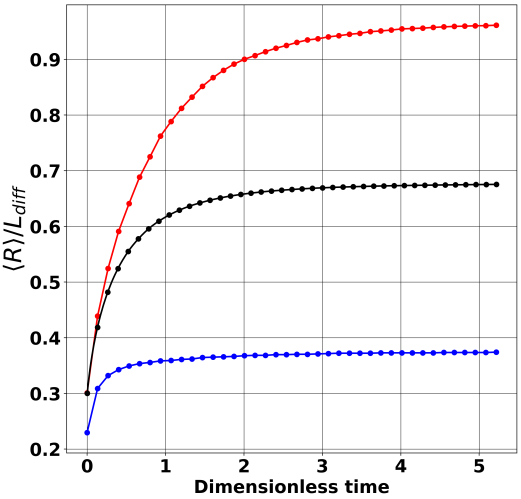

Figure 6. Evolutions of the grain envelope radius of the grain inside the largest Voronoi cell (red), the grain inside the smallest cell (blue) and the overall average (black). These extractions are for the low grain density simulation.

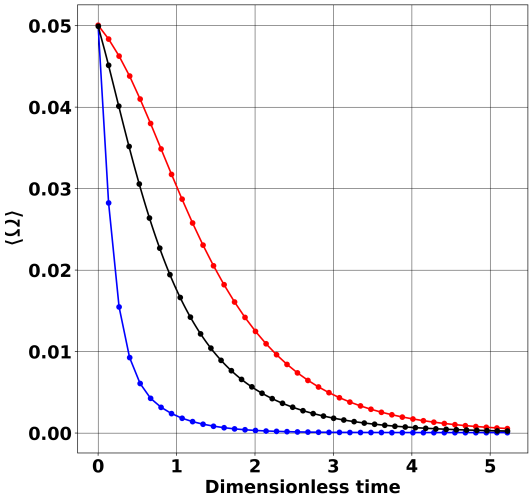

Figure 7. Evolutions of the average supersaturation in the extragranular liquid inside the largest Voronoi cell (red), inside the smallest cell (blue) and the global average in the system (black). These extractions are for the low grain density simulation.

4.3. The origin of the disparity between periodic and random grain arrangements

Figure 8 illustrates the distribution of Voronoi cell sizes in a random arrangement through a histogram. The vertical dashed lines divide the histogram into five classes, each representing one fifth of the total number of cells (125). The volume occupied by cells in each class is shown in red at the top of the figure. The results show that the largest 20% of cells in the distribution occupy around 37% of the total volume of the system, while the smallest 20% of cells only occupy 8% of the total volume. It should be noted that larger cells take longer to reach equilibrium, as shown in Figure 7. This means that a larger fraction of the total volume of the random system is occupied by large cells, which exhibit slow decrease in supersaturation, compared to small cells that reach equilibrium quickly.

Therefore, the overall behavior of the random ensemble is primarily influenced by the larger cells. Additionally, the average grain radius in the random arrangement takes longer to reach its final size compared to the periodic arrangement. This can be attributed to the long time needed by the large cells to reach equilibrium, despite the faster growth rate in large cells due to weaker interactions. Because the large cells are dominant in the random arrangement, this prolongs the driving force for growth of the ensemble.

5. Comparison with mean-field models

Mean-field models are commonly used in simulating phenomena at the process scale due to their low computational cost compared to full-field models. However, these models are based on simplifying assumptions that can compromise the accuracy of predictions. One such assumption is that they represent a population of grains with a single average grain. Additionally, grain interactions are described using a simplified description of solute diffusion around the grains. One of the goals of the present study is to demonstrate the limitations of mean-field models of

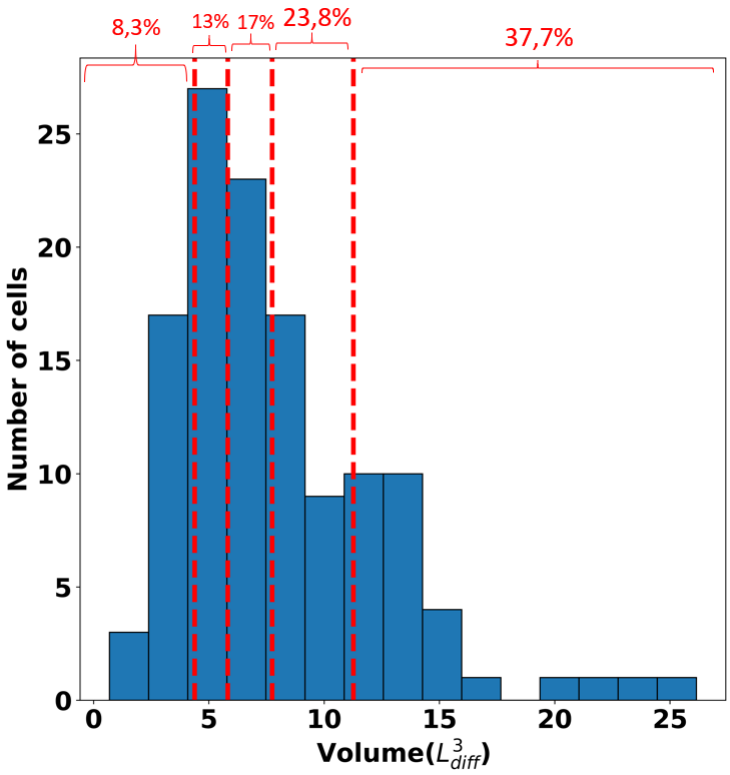

Figure 8.
Distribution of Voronoi cell sizes in the random grain distribution for low grain density. The vertical dashed lines in the graph divide the data into five classes, with each class containing 1/5 of the total number of cells. The volume occupied by the cells in each class is presented at the top of the graph.

equiaxed grain growth that result from the lack of descriptors for grain arrangement.

We compare the evolution of the global grain envelope fraction obtained by the full-field GEM simulations in isothermal conditions with predictions from two mean-field models for equiaxed solidification (Fig. 9). The "Classical model", proposed by Bedel et al. [8], is based on the so-called three-phase model of Wang & Beckermann [4], with an enhancement in terms of the constitutive relation for solute diffusion length in the extragranular liquid. The three phases are the solid, the intragranular liquid (assumed at equilibrium), and the extragranular liquid (considered supersaturated), where the two liquids are separated by the dendrite envelope. The solute exchange between the phases is described by volume-averaged solute balances at the interfaces. The model thus uses similar concepts as the GEM, but describes everything in a volume-averaged sense. Major assumptions in the constitutive relations are that: (i) the envelope has a fixed octahedral shape; (ii) the diffusion flux from the envelope to the extragranular liquid is approximated from an analytical solution of the concentration field around a sphere growing in a closed spherical domain, (iii) the envelope velocity is calculated from an LGK-type model of a freely growing dendrite tip, approximating the far-field concentration by the the average concentration in the extragranular liquid.

The second mean-field model, referred to as the "Upscaled model", was proposed by Torabi Rad et al. [9]. The main concepts are the same as in the Classical model: volume-averaged description, three phases, interface balances. The key difference is that in the Upscaled

model the constitutive relations were obtained by upscaling from full-field GEM simulations. The upscaling was done by averaging over a simulated ensemble of equiaxed grains arranged periodically on a BCC lattice [9]. The upscaled constitutive relations describe: (i) the variation of the envelope sphericity during growth, (ii) a diffusion flux fitted to the full-field simulations, (iii) the dependence of the envelope velocity on an effective concentration, different from the extragranular concentration.

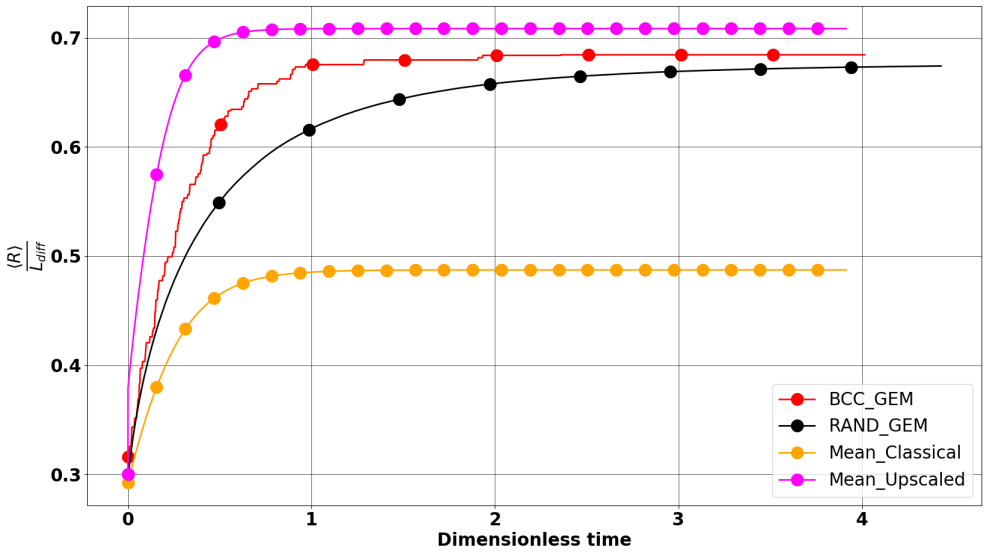

Figure 9. Comparison of evolutions of the equivalent envelope radius for the full-field GEM simulations with random arrangement (black) and BCC (red) arrangements, and for the Classical (orange) and Upscaled (magenta) mean-field models.

The comparisons of the two mean-field with full-field GEM simulations for random and BCC arrangements are shown in Fig. 9. The Classical mean-field model strongly underestimates both the growth rate and the final grain size. This shows that the assumptions contained in this model may be too simplistic to realistically reproduce growth. The Upscaled mean-field model provides a satisfactory prediction for the periodic BCC arrangement, however, it is unable to accurately simulate the growth of the random ensemble. This outcome is expected as the constitutive relations of this model were derived by upscaling simulations for BCC grain arrangements.

6. Conclusions and perspectives

Three dimensional numerical simulations for equiaxed grain growth were performed with a full-field model, for three periodic and for random grain arrangements. A major difference in terms of growth evolution was observed between periodic and random arrangements. Additionally, an investigation on the scale of the individual grains was carried out in order to explain the observations. Furthermore, a description of grain interactions was proposed and used to explain the results. Besides, a comparison with two mean-field models was performed showing the limitations of their predictions. Finally, the description of grains arrangement that we have proposed can pave the way for the enhancement of mean field grain growth models by integrating the grain arrangement and interactions aspect while keeping a reasonable computational cost.

Acknowledgement
The authors acknowledge the support by the French State through the program "Investment in the future" operated by the National Research Agency (ANR) and referenced by ANR-11 LABX-0008-01 (LabEx DAMAS). A part of the required high performance computing resources was provided by the EXPLOR center hosted by the Université de Lorraine.

References

[1] Murphy A, Mathiesen R, Houltz Y, Li J, Lockowandt C, Henriksson K, Zimmermann G, Melville N and Browne D 2016 *Journal of Crystal Growth* **440** 38–46
[2] Bogno A, Nguyen-Thi H, Reinhart G, Billia B and Baruchel J 2013 *Acta Materialia* **61** 1303–1315
[3] Rappaz M and Thevoz P 1987 *Acta Metallurgica* **35** 1487–1497
[4] Wang C and Beckermann C 1993 *Metallurgical and Materials Transactions A* **24** 2787–2802
[5] Steinbach I, Beckermann C, Kauerauf B, Li Q and Guo J 1999 *Acta Materialia* **47** 971–982
[6] Delaleau P, Beckermann C, Mathiesen R H and Arnberg L 2010 *ISIJ International* **50** 1886–1894
[7] Souhar Y, De Felice V F, Beckermann C, Combeau H and Založnik M 2016 *Computational Materials Science* **112** 304–317
[8] Bedel M 2014 *Étude de la formation des structures de solidification et des macroségrégations en coulée semi-continue d'aluminium* Ph.D. thesis université de Lorraine
[9] Torabi Rad M, Založnik M, Combeau H and Beckermann C 2019 *Materialia* **5** 100231